



Published in final edited form as:

Ophthalmology. 2016 June ; 123(6): 1222–1231. doi:10.1016/j.ophtha.2016.02.016.

Rectus Pulley Displacements Without Abnormal Oblique Contractility Explain Strabismus in Superior Oblique Palsy

Soh Youn Suh¹, Alan Le^{1,4,5}, Robert A. Clark^{1,6}, and Joseph L. Demer^{1,2,3,4,5,6}

¹Department of Ophthalmology, University of California, Los Angeles

²Stein Eye Institute, University of California, Los Angeles

³Department of Neurology, University of California, Los Angeles

⁴Neuroscience, University of California, Los Angeles

⁵Bioengineering Interdepartmental Programs, University of California, Los Angeles

⁶David Geffen Medical School, University of California, Los Angeles

Abstract

Purpose—Using high-resolution magnetic resonance imaging (MRI), we investigated whether rectus pulleys are significantly displaced in superior oblique (SO) palsy, and if displacements account for strabismus patterns.

Design—Prospective, case-control study.

Participants—Twenty-four patients diagnosed with SO palsy based on atrophy of SO muscle on MRI, and 19 age-matched orthotropic control subjects.

Methods—High resolution, surface coil MRI was obtained in multiple, contiguous, quasicoronal planes during monocular central gaze fixation. Pulley locations in oculocentric coordinates in the following subgroups of patients with SO palsy were compared with normal in subgroups of patients with SO palsy: unilateral vs bilateral, congenital vs acquired, and isotropic (round shape) vs anisotropic (elongated shape) SO atrophy. Expected effects of pulley displacements were modeled using *Orbit 1.8*® computational simulation.

Main outcome measures—Rectus pulley positions and ocular torsion.

Results—Rectus pulleys were typically displaced in SO palsy. In unilateral SO palsy, on average the medial rectus (MR) pulley was displaced 1.1 mm superiorly, the superior rectus (SR) pulley

The corresponding author is Joseph L. Demer, M.D., Ph.D. Stein Eye Institute, 100 Stein Plaza, UCLA, Los Angeles, California, 90095-7002 U.S.A. Phone: 310-825-5931, fax: 310-206-7826, ; Email: jld@jsei.ucla.edu

Address for Reprints, Joseph L. Demer, M.D., Ph.D., Stein Eye Institute, 100 Stein Plaza, UCLA, Los Angeles, California, 90095-7002 U.S.A., Phone: 310-825-5931, Fax: 310-206-7826, jld@jsei.ucla.edu

Publisher's Disclaimer: This is a PDF file of an unedited manuscript that has been accepted for publication. As a service to our customers we are providing this early version of the manuscript. The manuscript will undergo copyediting, typesetting, and review of the resulting proof before it is published in its final citable form. Please note that during the production process errors may be discovered which could affect the content, and all legal disclaimers that apply to the journal pertain.

Meeting presentation: Accepted for presentation at American Association for Pediatric Ophthalmology and Strabismus (AAPOS) Annual Meeting, April 7, 2016.

Conflict of Interest: No conflicting relationship exists for any author.

0.8 mm temporally, and the inferior rectus (IR) pulley 0.6 mm superior and 0.9 mm nasal from normal. Displacements were similar in bilateral SO palsy, with SR pulley additionally displaced 0.9 mm superiorly. However, the lateral rectus (LR) pulley was not displaced in either unilateral or bilateral SO palsy. The SR and MR pulleys were displaced in congenital SO palsy, while the IR and MR pulleys were displaced in acquired palsy. Pulley positions did not differ between isotropic and anisotropic palsy, or between patients with cyclotropia $<7^\circ$ versus 7° . Simulations predicted that the observed pulley displacements alone could cause patterns of incomitant strabismus typical of SO palsy, without requiring any abnormality of SO or inferior oblique strength.

Conclusion—Rectus pulley displacements alone, without abnormal oblique muscle contractility, can create the clinical patterns of incomitant strabismus in SO palsy. This finding supports accumulating evidence that clinical binocular misalignment patterns are not reliable indicators of contractile function of the SO muscle. Ocular torsion does not correlate with and thus cannot account for pulley displacements in SO palsy.

The directions of forces exerted by the extraocular muscles (EOMs) are determined by the connective tissue pulleys through which the EOMs transit: thus, EOM force vectors are determined by pulley positions.^{1–4} While magnetic resonance imaging (MRI) has shown that pulley positions are quite uniform among normal people,^{2, 5} abnormalities of rectus pulley positions are consistently associated with incomitant strabismus that may simulate oblique EOM dysfunction.^{6, 7} For example, infero-lateral displacement of lateral rectus (LR) pulley caused by connective tissue involution in sagging eye syndrome has recently been recognized as a cause of age-related distance esotropia and hypertropia in older people.⁸

Rectus pulley positions in the coronal plane are normally subject to the actions of the orbital layers of the oblique EOMs, and consequently shift by modest amounts under physiologic conditions.^{9–11} For example, the array of the four rectus pulleys rotates in torsional fashion around the long axis of the orbit during ocular counter-rolling¹² and during convergence¹³, paralleling the direction and amount of the corresponding physiologic ocular torsion. It seems plausible that cyclovertical strabismus, commonly associated with oblique EOM dysfunction, might alter rectus pulley positions. An MRI study has demonstrated abnormal pulley shifts during head tilt in subjects with head tilt dependent hypertropia (HTDHT) both with and without superior oblique (SO) muscle atrophy.¹⁴ Unlike physiologic ocular counter-rolling, the LR and inferior rectus (IR) pulleys paradoxically shifted into intorted positions in orbits having SO atrophy. In HTDHT without SO atrophy, the LR, medial (MR), and superior rectus (SR) pulleys in the hypertropic orbit exhibited reduced or reversed extorsional shift during head tilt. These differences in pathologic pulley shifts suggest that pulleys might contribute to the development of HTDHT, and that this contribution might be influenced by the presence of SO atrophy.

A monkey model of SO palsy produced by intracranial trochlear neurectomy has, by both histological and MRI criteria, confirmed that SO denervation reduces maximum SO cross section to about half of normal, and does so within five weeks.^{15–18} Since comparable SO atrophy and loss of contractile enlargement on infraduction are unequivocal evidence of human SO palsy, the MRI finding of SO atrophy can be regarded as a sufficient (albeit perhaps not a necessary) objective confirmation of the diagnosis of SO palsy.^{14, 18–20} This

confirmatory criterion makes sense because EOM size correlates well with contractile function^{15, 17, 20, 21}, so a markedly atrophic SO cannot generate normal force. Using the criterion of SO atrophy for unequivocal diagnosis of SO palsy, clinical series have demonstrated that the 3-step test is only 70% sensitive and 50% specific.¹⁸ Poor reliability of the 3-step and other time-honored clinical tests for diagnosis of SO weakness implies that strabismus practice may be confounded by inclusion of other pathologies "masquerading" as SO weakness.^{6, 7, 22, 23} Therefore, it has become important to evaluate the features and associations of actual SO weakness, rather than risking the perils of circular reasoning resulting from defining SO palsy as equivalent to a set of clinical motility findings that we now know are only occasional and inconsistent associations of palsy. An important validating role for orbital MRI has thus emerged.

In our earlier, small study, only the MR pulley was significantly displaced in patients with SO palsy.²⁴ However, biomechanical modeling suggested that displacement of the MR pulley alone could not cause the clinical patterns of strabismus observed in SO palsy. Moreover, the earlier MRI study suggested that isolated MR pulley displacement was unlikely to be a secondary effect of ocular excyclotorsion, since any ocular torsion should have displaced all the rectus pulleys to the same degree; none of the other three rectus pulleys were displaced.

The present study reinvestigates pulley positions in SO palsy in a substantially larger number of patients, and in several common subtypes of SO palsy. In light of the recent finding that the trochlear nerve bifurcates to separately innervate medial vs. lateral compartments of the SO muscle that are specialized for vertical vs. torsional actions,²⁵ a novel classification has been proposed based on the shape of the palsied SO muscle: isotropic atrophy with rounded SO muscle cross section, vs. anisotropic atrophy with elongated SO muscle cross section.²⁶ It has also been suggested that the anatomic features of congenital vs. acquired SO palsy may differ.²⁷⁻³⁰ The present study analyzed pulley positions in unilateral vs. bilateral, congenital vs. acquired, and isotropic vs. anisotropic SO palsy, and investigated by computational simulation if any associated rectus pulley displacements might influence the clinical patterns of strabismus observed in SO palsy.

Methods

Subjects

We studied 24 cases (17 male and 7 female) of SO palsy and 19 age-matched, healthy, orthotropic control subjects (10 male and 9 female). Hypertropic subjects were diagnosed as having SO palsy based on evidence of atrophy of one or both SO muscles on coronal plane MRI. Patients were excluded when there was a history of previous strabismus surgery or if they had additional causes of strabismus such as dissociated vertical deviation, orbital trauma, or thyroid ophthalmopathy. The diagnosis of congenital or acquired SO palsy was based on the history of the age that strabismus was first noted and early photographs when available. Probable causes of acquired SO palsy included cranial trauma, brain stem hemorrhage, and surgical manipulation causing trochlear nerve palsy. All other acquired cases were regarded as idiopathic. Three patients with SO palsy included in the previous study²⁴ were reanalyzed in this study using methods differing from the original ones. All

subjects gave written, informed consent according to a protocol approved by the University of California, Los Angeles Institutional Review Board that conformed to the tenets of the Declaration of Helsinki.

Control subjects underwent comprehensive eye examinations to verify normal corrected vision, binocular alignment, and stereoacuity. Patients with SO palsy underwent complete ophthalmic evaluation, including binocular alignment measured by alternate prism cover testing by turning or tilting the patient's head about 30° in cardinal gazes and head tilt positions, as well as ocular versions, and stereoacuity was measured by Titmus test. Deviations were neutralized by placing base-down prism in front of the hypertropic eye. Diagnostic occlusion was not performed. Subjective ocular torsion was measured by double Maddox rods when age appropriate. Confirmatory Hess screen testing was performed in patients consistently able to appreciate diplopia with normal retinal correspondence.

Magnetic Resonance Imaging

High-resolution T1 or T2 fast spin echo MRI was performed in each subject using a 1.5-T scanner (Signa; GE Health Care; Milwaukee, WI) and a facemask-mounted, dual-phased surface coil array (Medical Advances, Milwaukee, WI), as described in detail elsewhere.^{17, 20} Each orbit was imaged during monocular fixation by that eye in central gaze. Contiguous 2 or 3 mm thick quasicoronal images were obtained perpendicular to the long axis of the orbit, using a matrix of 256×256 pixels over a 6, 8, or 10 cm field of view, giving 234–390 μm in-plane resolution.

Analysis

Digital MRI images were processed using Adobe Photoshop (Adobe Systems, San Jose, CA, USA), and were quantified using the program *Image J* (W. Rasband, National Institutes of Health, Bethesda, Maryland). Images of left orbits were reflected to the orientation of right orbits to analyze EOM positions uniformly.

Cross sections of the rectus and SO EOMs were manually outlined in contiguous images, and the area centroid was taken as the EOM position. The globe was assumed spherical and its 3-D center determined as previously described.⁵ Centroids of rectus EOMs in each plane were translated relative to a 3-D coordinate origin at the computed globe center, defining as positive the lateral, superior, and anterior directions.⁵ EOM path data were rotated to normalize the vertical, horizontal, and torsional orientation, referencing the interhemispheric fissure of the brain and the junction of the superior ethmoid sinus and the orbit as described previously.⁵

The SO was also manually outlined and the cross sectional area of the EOM was measured using the “area” function of *Image J* (Fig. 1). The area of the SO was measured sequentially in contiguous image planes to identify the image plane containing the maximum cross-sectional area.

The diagnosis of SO palsy was based on the maximum SO cross-sectional area and the ratio of palsied to fellow maximum SO cross-sectional area on MRI. Unilateral SO palsy was diagnosed when the ratio of palsied to fellow SO muscle size fell below the 95% confidence

interval of the ratios in normal subjects. Bilateral SO palsy was diagnosed when both SO muscle sizes were below the 95% confidence intervals of normal subjects.

To determine the shape of the palsied SO muscle, an ellipse was automatically fit to the SO cross section manually outlined in the image plane containing the globe-optic nerve junction, and the major and minor axes of the ellipse were automatically determined. Cross sections of the SO having major axis length less than 3.9 mm were considered to represent isotropic atrophy, while major axis length at least 3.9 mm were considered to represent anisotropic atrophy; this criterion is consistent with post hoc discriminant analysis published elsewhere.²⁶

Simulations of binocular alignment were performed using the *Orbit 1.8* digital computer model (Eidactics, San Francisco, CA, USA)³¹ using measured locations of rectus pulleys. To simulate SO palsy, SO contractility was additionally reduced to zero, and elastic strength of the SO was reduced to 50% of normal for the affected eye in unilateral SO palsy and for both eyes in bilateral SO palsy. No other EOM abnormalities were assumed in the simulations.

Main outcome measures were rectus EOM pulley positions in subjects with SO palsy and with controls. Sub-analysis comparisons were also made between unilateral vs. bilateral, congenital vs. acquired, and isotropic vs. anisotropic cases with SO palsy. In addition, pulley positions were correlated with binocular alignment measurements. Statistical analysis was performed with the Mann-Whitney test for comparing median values of clinical data and Student's *t* test for comparing mean values of pulley positions using GraphPad Prism (GraphPad Software, La Jolla, CA, USA).

Results

The median age of patients with SO palsy was 34 years (range, 1–83 years), closely matching that of normal subjects at 27 years (range, 18–74 years, $P = 0.89$).

Clinical findings

Nineteen patients had unilateral SO palsy and 5 patients had bilateral SO palsy. The median ages of patients with unilateral and bilateral SO palsy were 35 (range, 1–80) and 31 years (range, 5–83), respectively ($P=0.93$). Fifteen patients with unilateral and 3 with bilateral SO palsy experienced binocular diplopia, and 15 patients with unilateral and 2 patients with bilateral SO palsy exhibited compensatory head tilt. Median symptom duration was 4 years (range, 0.2–28) in unilateral SO palsy and 6 years (range, 0.5–20) in bilateral SO palsy ($P=0.69$). Ten patients with unilateral and 3 patients with bilateral SO palsy were able to compensate for their deviations in certain gaze positions or with head tilt. Stereoacuity was measured in 21 patients, and was measurable in 14 patients with unilateral and 2 patients with bilateral SO palsy. In unilateral SO palsy, the Titmus stereo fly could be perceived by 3 patients, and the median stereoacuity in 11 patients was 50 arcsec (range, 40–200). In bilateral SO palsy, one patient had 100 arcsec, and the other patient had 400 arcsec stereoacuity.

Palsy was congenital in 6 and acquired in 18 cases. The median age of patients with congenital SO palsy was 15 years (range, 1–22), significantly less than in acquired SO palsy at 46 years (range, 5–83, $P=0.002$). Median symptom duration was 15 years (range, 0.8–21) in congenital and 4 years (range 0.2–28) in acquired SO palsy ($P=0.13$).

Unilateral SO Palsy

In unilateral SO palsy, 5 cases were congenital and 14 patients acquired. Table 1 compares median values of hyperdeviation and torsion between congenital and acquired SO palsy. Deviations were generally larger in congenital than acquired palsy, but this was significant only for hypertropia in supraversion and contralesional lateral gaze.

Bilateral SO Palsy

Of the bilateral cases, 1 was congenital and 4 acquired. Median hypertropia in central gaze, supraversion, and infraversion was 5 (range, 0–8), 2 (range, 0–8), and 9 (range, 0–10), respectively. The median absolute difference in hypertropia between dextroversion and levoversion was 8 (range, 0–41). The median absolute difference in hypertropia between right and left head tilts was 8 (range, 0–34), and median excyclotorsion in the upright position was 20° (range, 0–20°). None of the foregoing clinical features differed significantly between unilateral and bilateral SO palsy ($P > 0.3$).

SO Size

Maximum cross-sectional area of the unilaterally palsied SO was $10.0 \pm 3.4 \text{ mm}^2$ (mean \pm standard deviation), approximately half that of the fellow SO, $19.5 \pm 3.3 \text{ mm}^2$, and the normal control SO, $18.9 \pm 2.7 \text{ mm}^2$ (Fig. 2, $P < 0.001$ for both). The maximum cross-sectional area of the SO contralateral to the palsy did not significantly differ from normal ($P = 0.42$). The ratio of palsied to fellow SO cross section was 0.51 ± 0.15 in unilateral palsy, much less than the ratio of smaller to larger SO cross section in normal control subjects, 0.93 ± 0.05 ($P < 0.001$). Maximum cross-sectional area of the bilaterally palsied SO was $9.1 \pm 3.8 \text{ mm}^2$, significantly subnormal ($P < 0.001$) but not significantly smaller than in unilateral palsy ($P = 0.54$, Fig. 2).

Maximum SO cross-sectional areas were compared between 5 congenital and 14 acquired cases of unilateral palsy (Fig. 3). Maximum cross-sectional area of the congenitally palsied SO was $7.1 \pm 2.1 \text{ mm}^2$, significantly less than both that of the fellow SO, $17.1 \pm 2.4 \text{ mm}^2$, and the normal control ($P < 0.002$). Likewise, maximum cross-sectional area of the acquired, palsied SO was $11.0 \pm 3.3 \text{ mm}^2$, significantly less than both that of the fellow SO, $20.4 \pm 3.2 \text{ mm}^2$, and the normal control ($P < 0.001$ for both). Maximum cross-sectional area of the fellow SO contralateral to unilateral congenital or acquired palsy did not significantly differ from normal. The congenitally palsied SO was significantly smaller than that in acquired palsy ($P = 0.02$). The size of the contralateral fellow SO did not differ significantly in congenital vs. acquired unilateral palsy.

SO shape

Based on shape of the palsied SO, 5 patients were determined to have isotropic atrophy and 14 to have anisotropic atrophy. Major axis length of the palsied SO in the isotropic atrophy

group was 3.3 ± 0.2 mm, which was significantly less than in the anisotropic atrophy group at 5.0 ± 0.1 mm ($P < 0.001$). The minor axis of the palsied SO did not differ significantly between the groups, 1.7 ± 0.2 mm in the isotropic and 2.3 ± 0.2 mm in the anisotropic atrophy group.

Rectus pulley positions

In unilateral SO palsy, the ipsilesional medial rectus (MR) pulley was displaced an average of 1.1 mm superiorly, the superior rectus (SR) pulley was displaced 0.8 mm temporally, and the inferior rectus (IR) pulley was displaced 0.8 mm nasally and 0.6 mm superiorly relative to normal controls ($P < 0.05$ for all, Fig. 4-A). However, the lateral rectus (LR) pulley not abnormally displaced. Contralesional pulleys in unilateral palsy were normally located.

In bilateral SO palsy, the MR pulley was displaced in each orbit an average of 1.5 mm superiorly, the SR pulley was displaced 2.0 mm laterally and 0.9 mm superiorly, and the IR pulley was displaced 0.9 mm nasally relative to normal controls ($P < 0.05$, Fig. 4-B). As in unilateral SO palsy, the LR pulley was not displaced from normal. Horizontal position of the SR pulley was significantly more laterally displaced in bilateral than in unilateral SO palsy ($P < 0.05$).

Ipsilesional rectus pulley positions were compared in congenital and acquired SO palsy (Fig. 5). In congenital palsy, the MR pulley was shifted 0.9 mm superiorly, and the SR pulley was shifted 1.3 mm temporally relative to normal ($P < 0.05$), while the IR and LR pulleys were not significantly displaced. In acquired palsy, the MR pulley was shifted 1.0 mm superiorly, and the IR pulley shifted 1.1 mm nasally and 0.7 mm superiorly relative to normal ($P < 0.05$), while the SR and LR pulleys were not significantly displaced. Contralesional eye pulley positions were similar in congenital and acquired SO palsy. Rectus pulley positions were compared in isotropic atrophy and anisotropic atrophy (Fig. 6), but none differed significantly in either ipsilesional or contralesional orbits.

Patients were divided into two groups according to degrees of excyclotorsion to investigate the effect of torsion on rectus pulley positions in unilateral SO palsy. The mean value 7° was taken as a discriminant that divided these patients into two groups of nearly equal numbers. There were no differences in mean ipsilesional rectus pulley positions between patients with torsion $< 7^\circ$ versus 7° ($P > 0.05$, Fig. 7).

Orbit 1.8® computational simulation was performed initially using the mean pulley locations measured in unilateral and bilateral SO palsy (simulation denoted Sim 1). Without postulating any SO weakness or abnormalities, pulley displacements observed in SO palsy alone were sufficient to simulate the clinical pattern of incomitant strabismus observed in SO palsy, including incomitant hypertropia and V-pattern esotropia (Fig. 8-A, B). Simulation of inferior oblique (IO) overaction by increasing IO strength to 150% of normal had little effect on binocular alignment, so this change was not included in other simulations. V-pattern strabismus, with greater esotropia in deorsumversion than in sursumversion, was more prominent in simulations of bilateral than unilateral palsy. In a second stage of simulation that combined pulley displacements with SO muscle weakness (simulation denoted Sim 2), simulated hypertropia in infraversion slightly increased, but the incomitance

pattern did not change appreciably for either unilateral or bilateral SO palsy (Fig. 8-C, D). Simulated binocular alignments did not differ significantly between congenital and acquired SO palsy nor between isotropic and anisotropic palsy.

Clinical alignment data were compared with the simulation results. In both unilateral and bilateral SO palsy, simulated deviations underestimated the hypertropia in central gaze. In unilateral SO palsy, mean measured hypertropia was 10.2°, which was larger than the Sim 1 result at 2.3° and Sim 2 result at 4.7°, respectively. In bilateral SO palsy, the measured hypertropia was 4.5° compared with simulated deviations of 0.2° by Sim 1 and 0.3° by Sim 2, respectively. The non-zero simulated central gaze deviations in bilateral palsy are due to computational round-off errors, since the simulated pathologies were symmetrical; the resulting angles of strabismus would be clinically indistinguishable from zero. While the general patterns of incomitance are similar, the absolute differences in central gaze hypertropia between simulations and observations may reflect inaccuracies within the simulation program or additional pathologies beyond pulley heterotopy and SO weakness that were not simulated. Such additional pathological changes could include compensatory changes in the contractile behavior of one or multiple EOMs.

Magnitudes of lateral incomitance and V-pattern in SO palsy, however, were overestimated by the computational simulations. Lateral incomitance is defined to be the difference in hypertropia between the contra- and ipsilesional directions as measured clinically and between the corresponding 30° horizontal eccentricities in simulations. In unilateral palsy, measured lateral incomitance of hypertropia was 11.4°, which was smaller than the Sim 1 prediction of 14.4° and the Sim 2 prediction of 17.2°. The measured difference in esodeviation between infraversion and supraversion (V-pattern) was 2.6°, which was again smaller than the simulated difference in esodeviation of 14.9° by Sim 1 and 18.1° by Sim 2. In bilateral SO palsy, measured lateral incomitance of hypertropia was 11.5°, which was smaller than the Sim 1 result at 25.3° and Sim 2 result at 35.0°, respectively. The measured difference in esodeviation between infraversion and supraversion (V-pattern) in bilateral SO palsy was 7.3°, versus the simulated difference in esodeviation of 25.3° by Sim 1 and 35.0° by Sim 2.

Discussion

This study demonstrates that rectus pulleys are often displaced in SO palsy and suggests that mechanical effects of these heterotopic pulley displacements alone can produce the clinical incomitance of strabismus considered typical of SO palsy. Although the displacements of individual pulleys were relatively small, computer simulation indicates that the combined effect of MR, SR, and IR pulley displacements, even without postulating abnormalities of SO muscle innervation or contractility, can explain the pattern of incomitant strabismus observed in SO palsy. Of course, additional compensatory innervational, mechanical, and contractile changes in one or multiple EOMs might also occur that are not considered in this study.

Rectus pulleys in patients with SO atrophy are displaced perpendicular to each EOM's plane of action (vertical for the MR and horizontal for the SR and IR pulleys), a phenomenon that

has been predicted to induce strabismus.² These displacements redirect rectus EOM forces into oblique directions. Large displacements of this kind are more likely than smaller ones to disrupt binocular alignment.⁶ The significantly greater lateral displacement of the SR pulley, combined with tendencies for greater displacement in the MR and IR pulleys, in bilateral SO palsy may explain the associated V-pattern and large excyclotorsion often observed clinically.³² In the current study, the clinical findings in unilateral and bilateral SO palsy did not significantly differ, perhaps due to small number of cases of bilateral SO palsy, or mixture of symmetrically and asymmetrically palsied bilateral cases.

Kono *et al.* have reported that rectus pulley displacements can simulate SO palsy in patients clinically diagnosed with SO palsy but who do not exhibit SO muscle hypoplasia or atrophy on MRI.⁷ Kono *et al.* showed that simulations based on heterotopic pulley positions alone predicted the actual patterns of strabismus better than simulations incorporating SO weakness alone. The current study confirms and extends the findings of Kono *et al.*, showing that simulated binocular alignment based on displaced pulleys alone was not substantially different from that predicted from displaced pulleys combined with SO weakness and loss of passive elasticity. These simulations suggest that the patterns of strabismus observed clinically in SO palsy primarily result from heterotopic rectus pulleys rather than from SO weakness. This result begs for fundamental reconsideration of the way SO palsy is understood clinically.

Both empirical studies in rhesus monkeys and theoretical studies using biomechanical modeling consistently suggest that SO muscle weakness alone is insufficient to explain the large hypertropia common in SO palsy.^{33–35} In the current study, even simulations based on pulley displacements with SO weakness underestimated the clinically measured hypertropia in both unilateral and bilateral SO palsy, but overestimated the V-pattern. These discrepancies between the clinical alignment data and simulation results imply contribution of other mechanisms besides SO weakness to clinical features of SO palsy. Neurally-mediated size and contractility changes of the contralesional vertical EOMs have been suggested as possible mechanisms underlying the large hypertropia associated with SO palsy.^{15, 21}

One might suppose that pulley displacements in SO palsy might be secondary to ocular excyclotorsion resulting from SO palsy.³⁶ However, the present study excludes this possibility. An MRI study of rectus pulley behavior during static ocular counter-rolling showed that the array of the rectus pulleys counter-rotates during head tilt.¹² If the excyclotorsion due to SO palsy were mechanically displacing the EOM pulleys, all four rectus pulleys should be systematically displaced in the same direction by similar amounts. Although MR, SR, and IR pulleys were here found to be slightly displaced in SO palsy, it is remarkable that the LR pulley, the pulley with the least stable connective tissue support,¹ was not displaced. Likewise, patients with SO palsy with greater excyclotorsion did not exhibit greater rectus pulley displacements than patients with lesser excyclotorsion.

Vertical rectus pulleys were displaced differently in congenital than in acquired SO palsy, but simulations suggested that this difference would not be reflected in significant differences in binocular alignment. However, the present study found the SO to be smaller in

congenital than in acquired SO palsy, confirming the report of Sato *et al.*²⁸ This difference in SO size may be due to the different etiologies, with the smaller SO in congenital palsy perhaps caused either by primary hypoplasia or by denervation atrophy,^{27, 29, 37, 38} but the latter perhaps the sole cause in acquired palsy.¹⁶

A recent study demonstrated two morphological types of SO palsy.²⁶ One type exhibited isotropic, rounded atrophy of the residual SO cross-section, while the other type showed anisotropic, elongated atrophy. The differing palsied SO shapes correlated with different strabismus patterns, including greater hypertropia in infraversion and greater excyclotorsion in anisotropic compared with isotropic SO atrophy. This difference may reflect the compartmental nature of the SO and its innervation by separate branches of the trochlear nerve: the medial SO compartment is selective for incycloduction and the lateral SO compartment for infraduction.²⁵ In the current study, we asked if presumed selective compartmental atrophy of the SO muscle might change rectus pulley positions differently, and found that pulley positions were similar in isotropic and anisotropic atrophy. Compartmental SO palsy therefore does not selectively alter rectus pulley positions.

Palsy of the SO is associated with MR, SR, and IR pulley displacements that alone can produce the patterns of incomitant strabismus considered typical of SO palsy. These displacements are not caused by ocular torsion, but probably contribute to the low specificity of clinical diagnosis of SO palsy, which is only about 50% when MRI atrophy is employed as the confirmatory finding.¹⁴ Since the clinical 3-step test is only about 70% sensitive to SO weakness as confirmed by atrophy on MRI,¹⁸ it must be concluded that patterns of incomitant strabismus are only tenuously related to actual SO function. In most cases, SO function cannot be assessed reliably by clinical evaluations of ocular motility and binocular alignment. These observations should motivate reconsideration of current diagnostic practices in strabismology.³⁹ For example, overelevation in adduction and underdepression in adduction can be seen in cases of actual SO muscle weakness, but these findings are hardly specific for the functions of particular oblique extraocular muscles, so the findings should be described as clinical observations rather than mechanistic conclusions. Clinical terms connoting implied diagnoses of particular pathophysiologic mechanisms, such as "superior oblique underaction" and "inferior oblique overaction," should therefore be avoided.

Acknowledgments

Funding/Support: This study was supported by grants to Joseph L. Demer from the U.S. Public Health Service (NEI grant EY008313), Washington, DC, and an unrestricted grant from Research to Prevent Blindness, New York, NY. The funding organization had no role in the design or conduct of this research.

References

1. Demer JL, Miller JM, Poukens V, et al. Evidence for fibromuscular pulleys of the recti extraocular muscles. *Invest Ophthalmol Vis Sci.* 1995; 36:1125–1136. [PubMed: 7730022]
2. Clark RA, Miller JM, Demer JL. Location and stability of rectus muscle pulleys. Muscle paths as a function of gaze. *Invest Ophthalmol Vis Sci.* 1997; 38:227–240. [PubMed: 9008649]
3. Demer JL, Oh SY, Poukens V. Evidence for active control of rectus extraocular muscle pulleys. *Invest Ophthalmol Vis Sci.* 2000; 41:1280–1290. [PubMed: 10798641]

4. Kono R, Clark RA, Demer JL. Active pulleys: magnetic resonance imaging of rectus muscle paths in tertiary gazes. *Invest Ophthalmol Vis Sci*. 2002; 43:2179–2188. [PubMed: 12091414]
5. Clark RA, Miller JM, Demer JL. Three-dimensional location of human rectus pulleys by path inflections in secondary gaze positions. *Invest Ophthalmol Vis Sci*. 2000; 41:3787–3797. [PubMed: 11053278]
6. Clark RA, Miller JM, Rosenbaum AL, et al. Heterotopic muscle pulleys or oblique muscle dysfunction? *J AAPOS*. 1998; 2:17–25. [PubMed: 10532362]
7. Kono R, Okanobu H, Ohtsuki H, et al. Displacement of the rectus muscle pulleys simulating superior oblique palsy. *Jpn J Ophthalmol*. 2008; 52:36–43. [PubMed: 18369698]
8. Chaudhuri Z, Demer JL. Sagging eye syndrome: connective tissue involution as a cause of horizontal and vertical strabismus in older patients. *JAMA Ophthalmol*. 2013; 131:619–625. [PubMed: 23471194]
9. Demer JL, Oh SY, Clark RA, et al. Evidence for a pulley of the inferior oblique muscle. *Invest Ophthalmol Vis Sci*. 2003; 44:3856–3865. [PubMed: 12939301]
10. Kono R, Poukens V, Demer JL. Quantitative analysis of the structure of the human extraocular muscle pulley system. *Invest Ophthalmol Vis Sci*. 2002; 43:2923–2932. [PubMed: 12202511]
11. Demer JL. Pivotal role of orbital connective tissues in binocular alignment and strabismus: the Friedenwald lecture. *Invest Ophthalmol Vis Sci*. 2004; 45:729–738. 8. [PubMed: 14985282]
12. Demer JL, Clark RA. Magnetic resonance imaging of human extraocular muscles during static ocular counter-rolling. *J Neurophysiol*. 2005; 94:3292–3302. [PubMed: 16033934]
13. Demer JL, Kono R, Wright W. Magnetic resonance imaging of human extraocular muscles in convergence. *J Neurophysiol*. 2003; 89:2072–2085. [PubMed: 12686579]
14. Demer JL, Kung J, Clark RA. Functional imaging of human extraocular muscles in head tilt dependent hypertropia. *Invest Ophthalmol Vis Sci*. 2011; 52:3023–3031. [PubMed: 21282574]
15. Clark RA, Demer JL. Enhanced vertical rectus contractility by magnetic resonance imaging in superior oblique palsy. *Arch Ophthalmol*. 2011; 129:904–908. [PubMed: 21746981]
16. Demer JL, Poukens V, Ying H, et al. Effects of intracranial trochlear neurectomy on the structure of the primate superior oblique muscle. *Invest Ophthalmol Vis Sci*. 2010; 51:3485–3493. [PubMed: 20164458]
17. Kono R, Demer JL. Magnetic resonance imaging of the functional anatomy of the inferior oblique muscle in superior oblique palsy. *Ophthalmology*. 2003; 110:1219–1229. [PubMed: 12799250]
18. Manchandia AM, Demer JL. Sensitivity of the three-step test in diagnosis of superior oblique palsy. *J AAPOS*. 2014; 18:567–571. [PubMed: 25459202]
19. Kono R, Okanobu H, Ohtsuki H, et al. Absence of relationship between oblique muscle size and bielschowsky head tilt phenomenon in clinically diagnosed superior oblique palsy. *Invest Ophthalmol Vis Sci*. 2009; 50:175–179. [PubMed: 18791177]
20. Demer JL, Miller JM. Magnetic resonance imaging of the functional anatomy of the superior oblique muscle. *Invest Ophthalmol Vis Sci*. 1995; 36:906–913. [PubMed: 7706039]
21. Jiang L, Demer JL. Magnetic resonance imaging of the functional anatomy of the inferior rectus muscle in superior oblique muscle palsy. *Ophthalmology*. 2008; 115:2079–2086. [PubMed: 18692249]
22. Kushner BJ. Errors in the three-step test in the diagnosis of vertical strabismus. *Ophthalmology*. 1989; 96:127–132. [PubMed: 2919044]
23. Donahue SP, Lavin PJ, Hamed LM. Tonic ocular tilt reaction simulating a superior oblique palsy: diagnostic confusion with the 3-step test. *Arch Ophthalmol*. 1999; 117:347–352. [PubMed: 10088812]
24. Clark RA, Miller JM, Demer JL. Displacement of the medial rectus pulley in superior oblique palsy. *Invest Ophthalmol Vis Sci*. 1998; 39:207–212. [PubMed: 9430565]
25. Le A, Poukens V, Ying H, et al. Compartmental innervation of the superior oblique muscle in mammals. *Invest Ophthalmol Vis Sci*. 2015; 56:6237–6246. [PubMed: 26426404]
26. Shin SY, Demer JL. Superior oblique extraocular muscle shape in superior oblique palsy. *Am J Ophthalmol*. 2015; 159:1169–1179. [PubMed: 25747676]

27. Yang HK, Kim JH, Hwang JM. Congenital superior oblique palsy and trochlear nerve absence: a clinical and radiological study. *Ophthalmology*. 2012; 119:170–177. [PubMed: 21924501]
28. Sato M, Yagasaki T, Kora T, et al. Comparison of muscle volume between congenital and acquired superior oblique palsies by magnetic resonance imaging. *Jpn J Ophthalmol*. 1998; 42:466–470. [PubMed: 9886737]
29. Helveston EM, Krach D, Plager DA, et al. A new classification of superior oblique palsy based on congenital variations in the tendon. *Ophthalmology*. 1992; 99:1609–1615. [PubMed: 1454330]
30. Sato M. Magnetic resonance imaging and tendon anomaly associated with congenital superior oblique palsy. *Am J Ophthalmol*. 1999; 127:379–387. [PubMed: 10218689]
31. Miller, JM.; Pavlovski, DS.; Shaemeva, I. *Orbit 1.8 ed.* San Francisco: Eidactics; 1999. Gaze Mechanics Simulation.
32. von Noorden GK, Murray E, Wong SY. Superior oblique paralysis. A review of 270 cases. *Arch Ophthalmol*. 1986; 104:1771–1776. [PubMed: 3789976]
33. Shan X, Tian J, Ying HS, et al. Acute superior oblique palsy in monkeys: I. Changes in static eye alignment. *Invest Ophthalmol Vis Sci*. 2007; 48:2602–2611. [PubMed: 17525190]
34. Miller JM, Robinson DA. A model of the mechanics of binocular alignment. *Computers and biomedical research, an international journal*. 1984; 17:436–470.
35. Robinson DA. Bielschowsky head-tilt test--II. Quantitative mechanics of the Bielschowsky head-tilt test. *Vision research*. 1985; 25:1983–1988. [PubMed: 3832624]
36. Guyton DL, Weingarten PE. Sensory torsion as the cause of primary oblique muscle overaction/underaction and A- and V- pattern strabismus. *Binocular Vis Eye Muscle Surg Q*. 1994; 9:209–236.
37. Chan TK, Demer JL. Clinical features of congenital absence of the superior oblique muscle as demonstrated by orbital imaging. *J AAPOS*. 1999; 3:143–150. [PubMed: 10428587]
38. Kim JH, Hwang JM. Absence of the trochlear nerve in patients with superior oblique hypoplasia. *Ophthalmology*. 2010; 117:2208–2213. [PubMed: 20570358]
39. Demer JL. Clarity of words and thoughts about strabismus. *Am J Ophthalmol*. 2001; 132:757–759. [PubMed: 11704038]

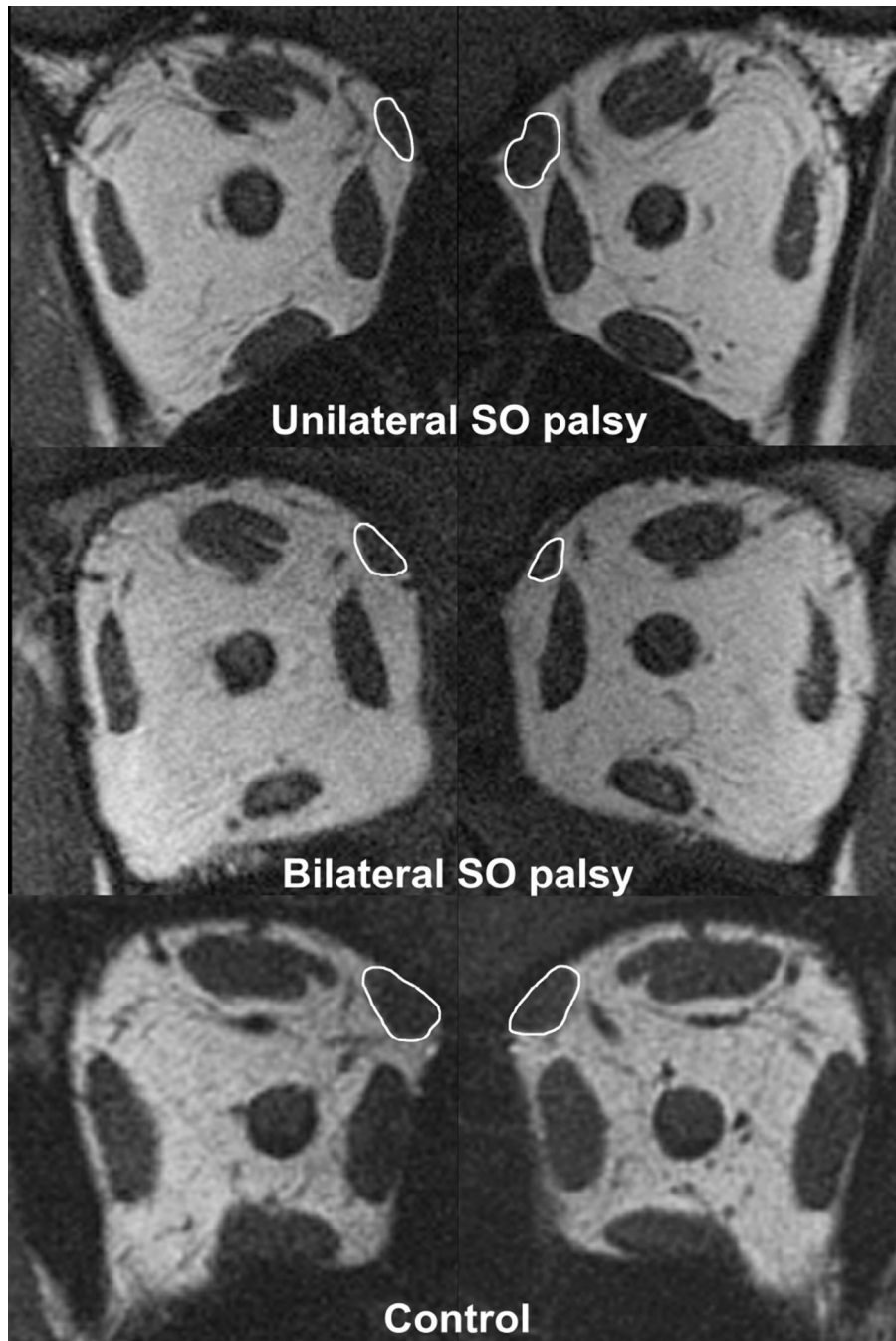


Fig. 1. Quasicoronal MRI of right (left column) and left (right column) orbits in patients with superior oblique (SO) palsy and a normal control. Note the smaller size of the right SO muscle compared with left SO muscle in unilateral SO palsy (top row). Both SO muscles are small in bilateral SO palsy (middle row).

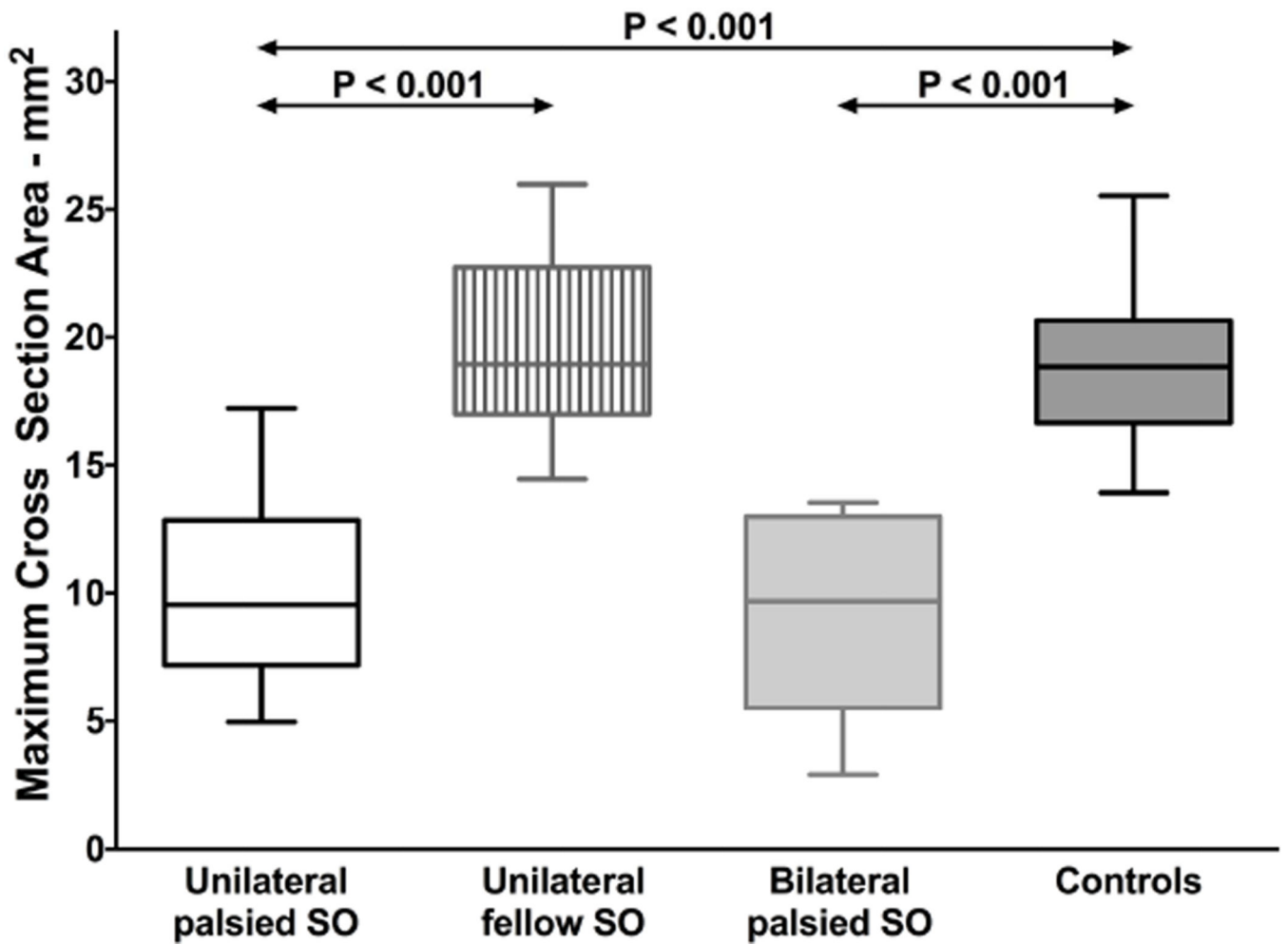


Fig. 2. Maximum cross-sectional area of the superior oblique (SO) muscle. Horizontal bars indicate median, rectangles the interquartile range, and error bars the minimum and maximum values.

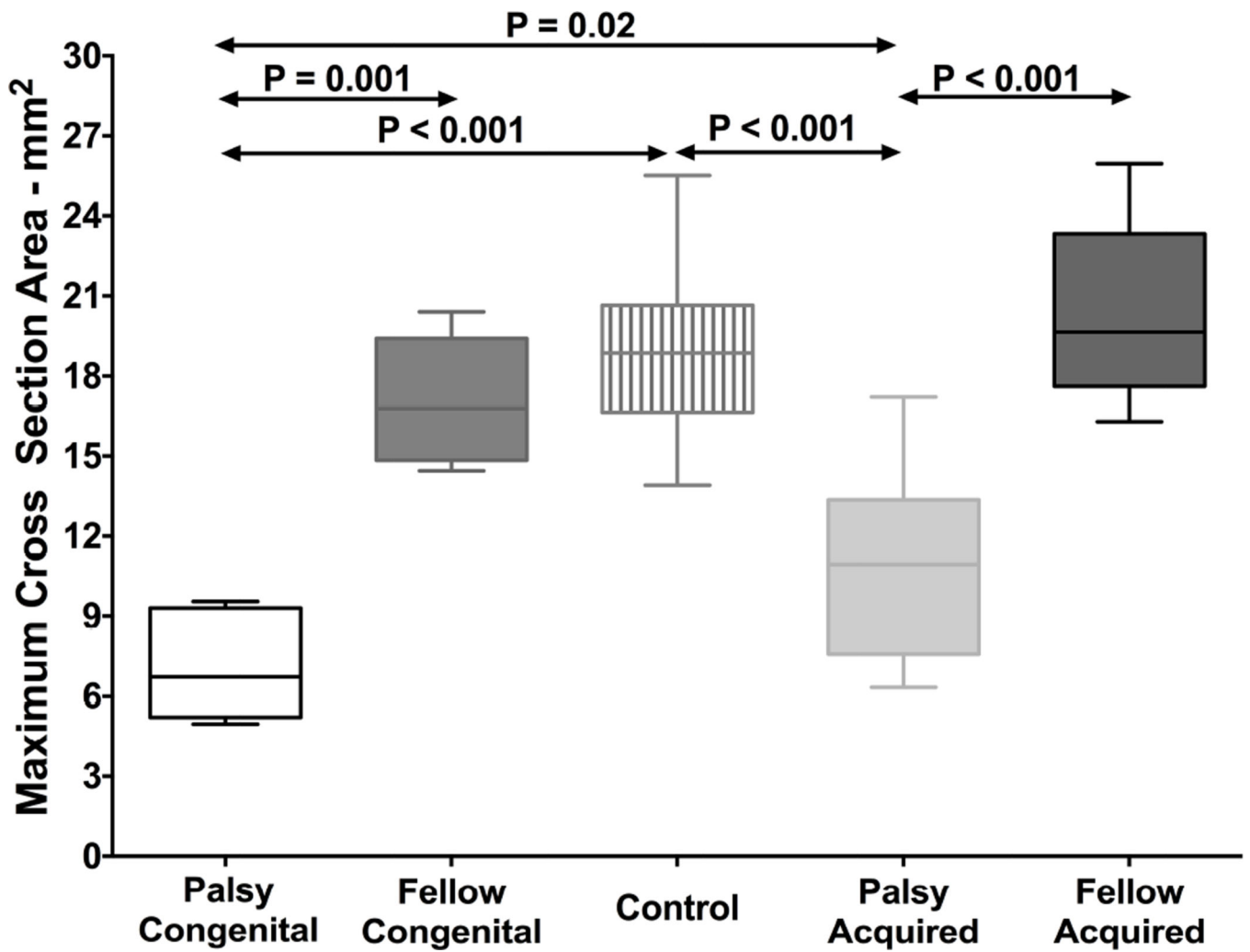


Fig. 3. Maximum cross-sectional area of the superior oblique muscle in congenital and acquired palsy. Horizontal bars indicate median, rectangles the interquartile range, and error bars the minimum and maximum values.

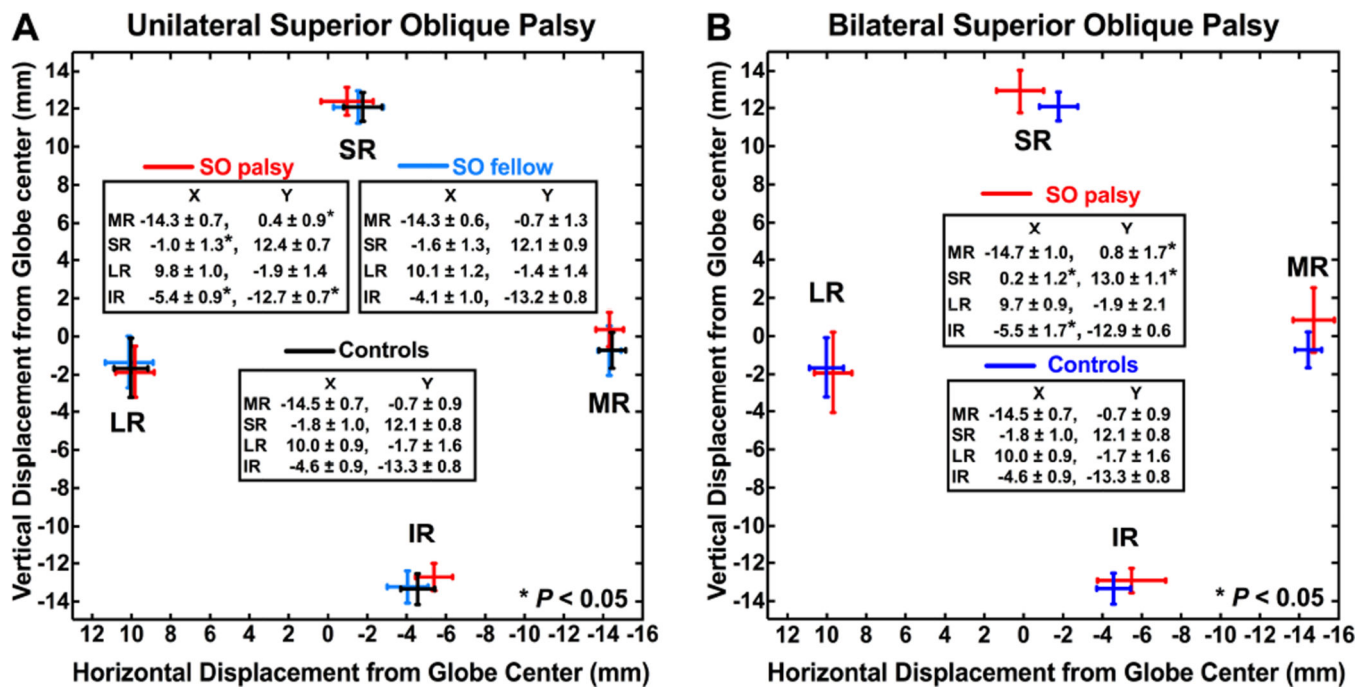


Fig. 4. Rectus pulley positions in (A) unilateral and (B) bilateral superior oblique palsy. Error bars shown represent 95% confidence intervals. Note the shifts of the medial, superior, and inferior rectus pulleys but not the lateral rectus pulley in both unilateral and bilateral palsy.

Congenital vs Acquired SO Palsy

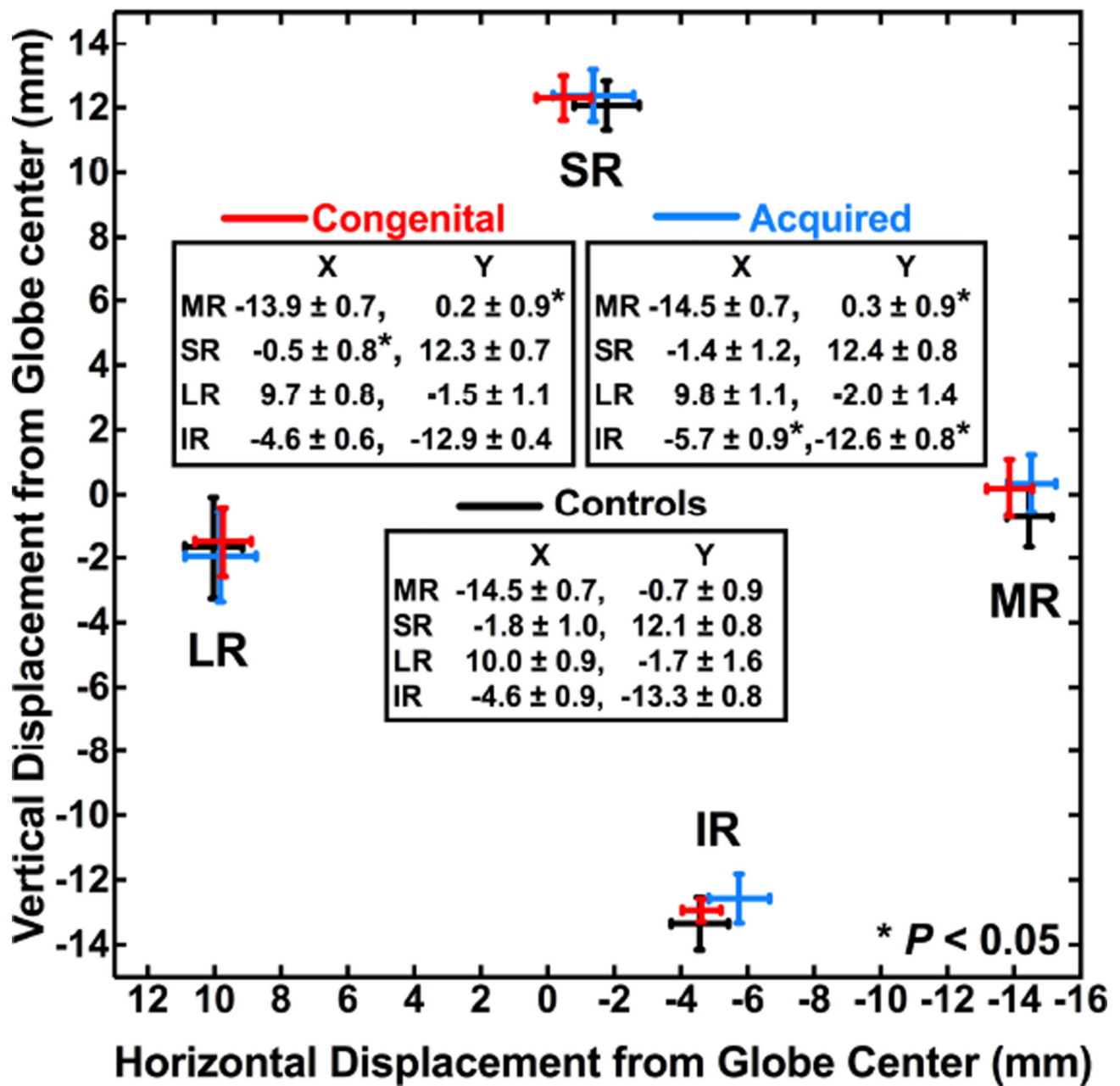


Fig. 5. Ipsilesional rectus pulley positions in congenital vs. acquired superior oblique (SO) palsy. Note shifts of the medial and superior rectus pulleys in congenital palsy, and the medial and inferior rectus pulleys in acquired palsy.

Isotropic vs Anisotropic SO palsy

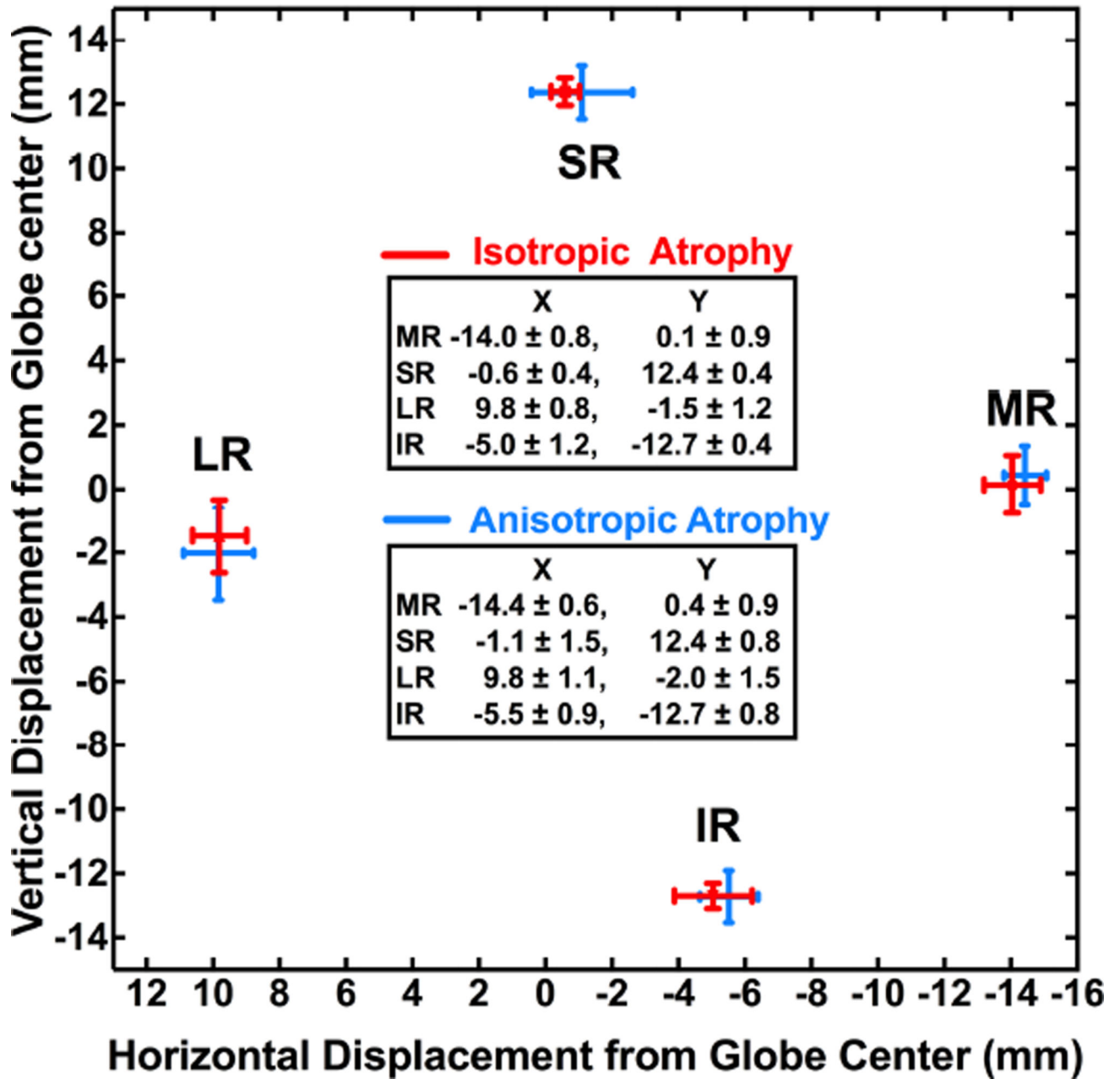


Fig. 6. Ipsilesional rectus pulley positions were similar in subjects with isotropic and anisotropic superior oblique (SO) atrophy.

Small Vs Large Extorsion

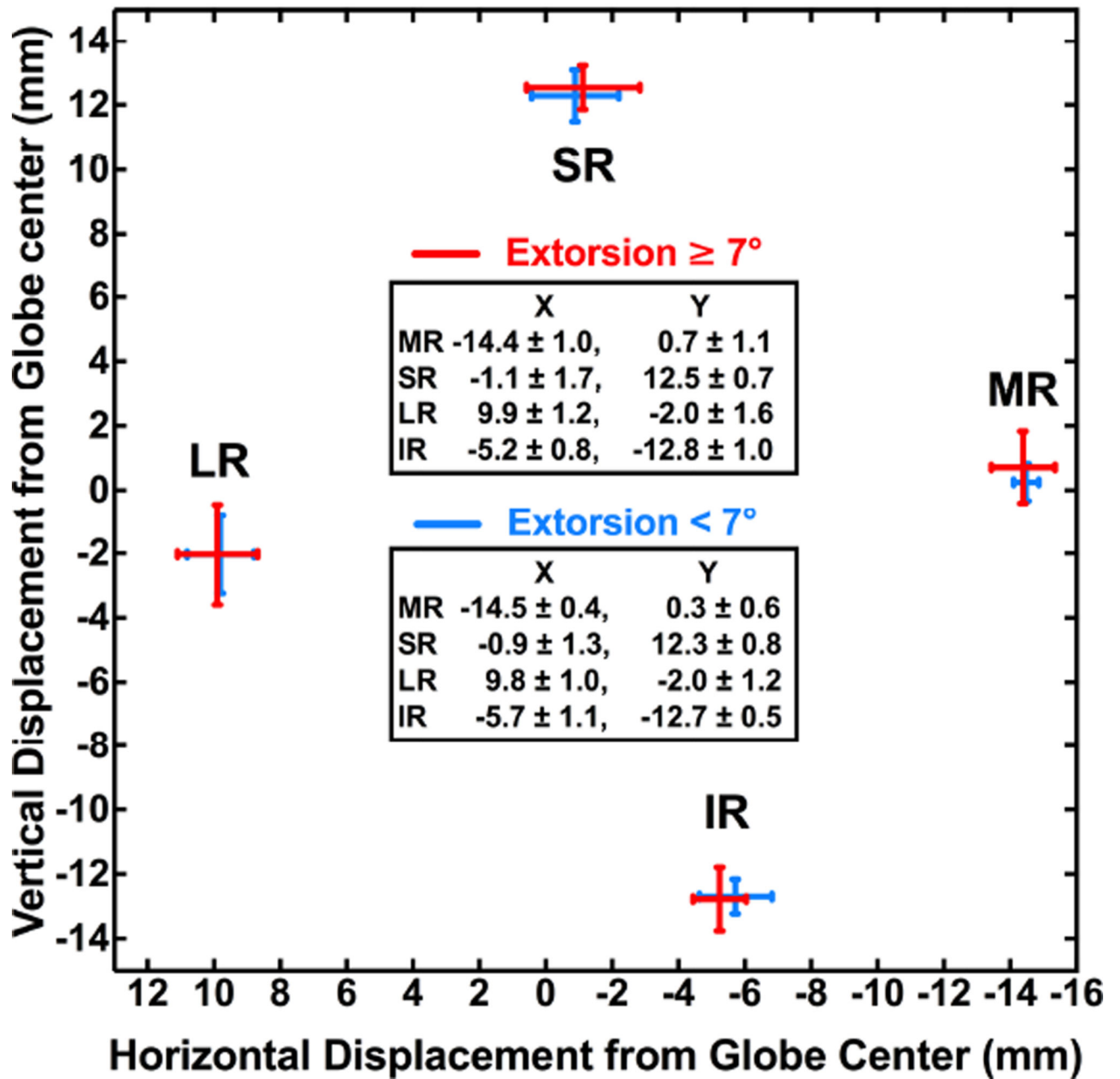


Fig. 7. Ipsilesional rectus pulley positions in unilateral superior oblique palsy in subjects with torsion <7° vs. 7°. There was no significant effect of larger vs. smaller ocular torsion on pulley positions.

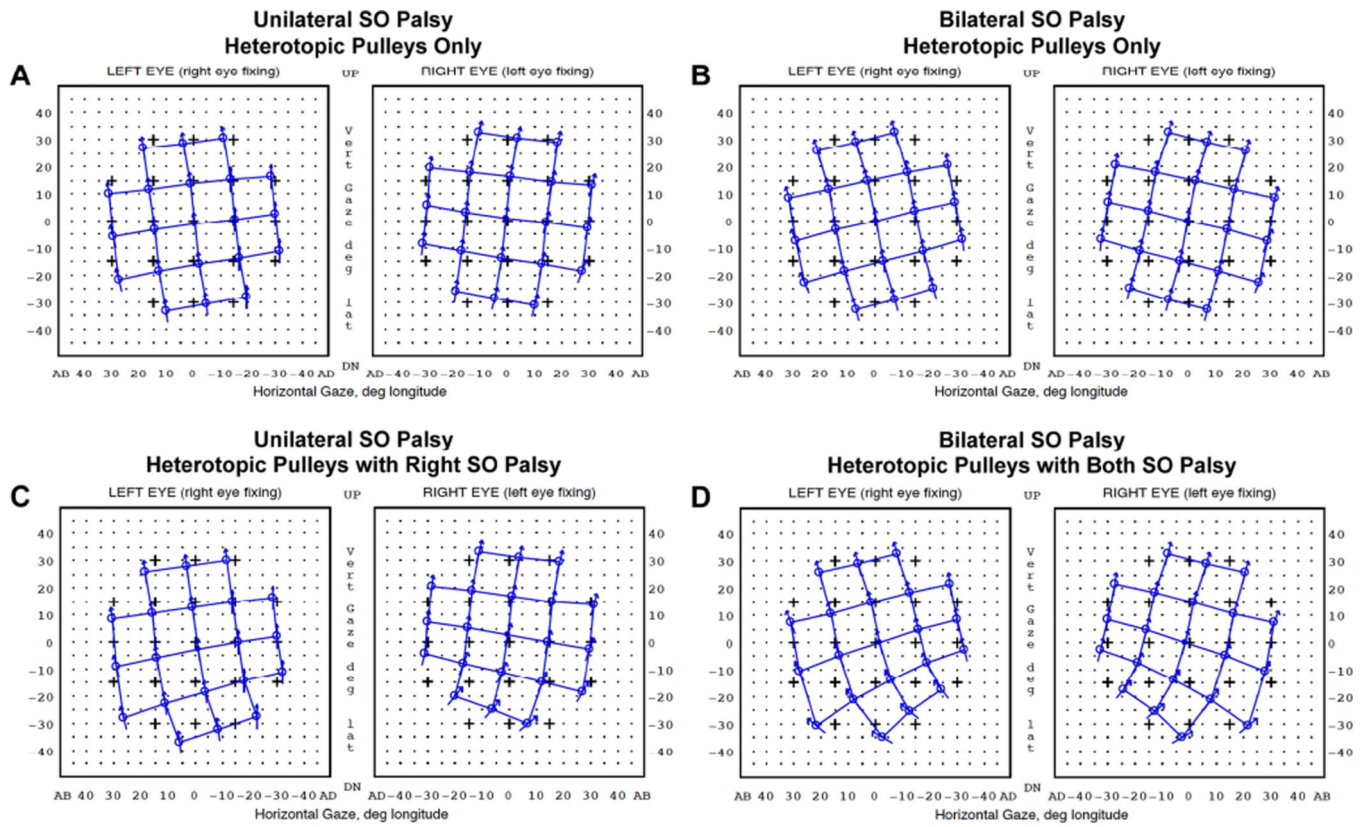


Fig. 8. *Orbit 1.8*[®] computational simulation in unilateral and bilateral superior oblique (SO) palsy. Hess screen charts shows the binocular alignment predicted from measured rectus pulley displacements alone (A, B), and combined with right SO weakness in unilateral (C) and bilateral weakness in bilateral SO palsy (D). SO weakness was simulated by reducing contractility to 0% and elastic strength to 50% of normal.

Table. 1

Binocular Alignment in Unilateral Superior Oblique Palsy

	Congenital (n=5)	Acquired (n=14)	P value
Hypertropia ()			
Central gaze	20 (0–37)	5 (2–18)	0.11
Supraversion*	14 (8–37)	5 (0–25)	0.01
Infraversion*	23 (12–37)	10 (0–30)	0.075
Lateral gaze*			
Ipsilesional	9 (6–35)	3 (0–30)	0.067
Contralesional	30 (20–42)	10 (1–30)	0.001
Head tilt			
Ipsilesional	30 (2–45)	10 (2–27)	0.073
Contralesional	0 (0–16)	0 (0–15)	0.96
Excyclotorsion (°) †	5 (5–7)	5 (0–25)	0.94

* Deviations in secondary gaze positions were not obtained in a one year old congenital case.

† Two congenital cases were too young to perform double Maddox rod testing.